# Vibrio Cholera: The Impacts of Anthropogenic Pollution on Biofilm Formation

**Meg Xu**

*Received December 31, 2024*
*Accepted April 12, 2025*
*Electronic access May 15, 2025*

Anthropogenic pollution alters natural environments, posing substantial risks to both ecosystems and human health. Notably, this pollution leads to a decrease in oceanic pH, contributing to the detrimental effects of acidification on marine life, exemplified by the development of bacterial biofilm. This review shows the effects of anthropogenic pollution using gram-negative bacterium *Vibrio Cholerae (Vc)*, the causative agent of cholera, as a model organism. *Vc* forms mature biofilms, resistant to external stressors on chitin surfaces by utilizing matrix components including Vibrio polysaccharides (VPS) and matrix proteins-RbmA, RbmC, Bap1. Previous research investigates the effects of pH on biofilm colony formation and bacterial growth in liquid culture, demonstrating that acidic conditions below a preferred pH of 8 can impede biofilm formation, resulting in notable reductions in mass and structural integrity. Furthermore, fluctuations in carboxyl and carbonyl groups due to an excess of H+ ions, coupled with the role of VPS structure in crosslinks with matrix proteins, suggests the correlation between acidity and VPS structure in *Vc*. This connection highlights the potential for environmental pH shifts to influence the epidemiology of cholera by affecting biofilm formation and stability, despite the potential of different *Vc* strains and environmental conditions to partially counteract trends demonstrated by changing acidity. This review provides an analysis of how pH variations impact biofilm formation and bacterial growth in *Vc*, emphasizing the importance of VPS in maintaining biofilm integrity. These insights contribute to a better understanding of the ecological and public health implications of pH fluctuations in aquatic environments.

**Keywords:** Vibrio Cholera, vibrio polysaccharides, biofilm formation, anthropogenic pollution, morphology, human population density, surface proteins

## Introduction

Increasing human activity and population density are drivers of anthropogenic pollution and the resultant surplus of CO2. Although the relationship between carbon emissions and demographic trends is a complex one, involving factors such as economic growth, previous studies demonstrate increasing CO2 emissions corresponding with upward trends in population density[1]. As atmospheric CO2 levels continue to increase, the chemical composition of the ocean, a major carbon sink, is being heavily altered[2]. The addition of excess carbon dioxide into the seawater reacts with H20, forming carbonic acid. Due to the weak and unstable nature of this acid, it then dissociates into bicarbonate and hydrogen ions. The acidic nature of these hydrogen ions triggers a decrease in the overall pH of seawater. Even slight changes in ocean acidity hold the potential to shape the behavior and survival of marine organisms[3]. For example, decreasing pH affects aqueous bacteria and related communities of microorganisms, ultimately leading to potential negative impacts on human health.

*Vc* is a gram-negative bacteria which lives primarily in aqueous habitats and is susceptible to the impacts of ocean acidification due to its acidity preference for pH 8 despite its ability to grow between pH 6.5 and 9[2].*Vc* is represented by over 200 serotypes, among which are the Classical 0139 and El Tor 01 strains responsible for previous and currently ongoing global cholera pandemics[2]. Previous estimates predict that there are up to 4 million cases of cholera yearly with outbursts located primarily in countries which have limited access to potable water[4].

*Vc* is among many bacterial species which utilize the production of biofilm in order to enhance resistance against stressful environmental factors. *Vc* biofilm is formed by a community of microorganisms which interact and attach with VPS in its self-produced biofilm matrix. *Vc* biofilm develops primarily on chitin surfaces in its natural aquatic habitat. Through the use of flagellar propulsion coded for by the flaA gene loci, *Vc* approaches and attaches to suitable surfaces[5]. Upon initial contact, reversible attachment is established, triggering the release of cyclic di guanosine monophosphate (c-di-GMP)[6]. In turn c-di-GMP is produced by DGCs(diguanylate cyclase) and regulated by PDEs(phosphodiesterase)[7]. The presence of sensory domains in many *Vc* DGCs/PDEs thus suggests the presence of external environmental cues, and the modulation of c-di-GMP

production through environmental parameters[7]. Thus, biofilm architecture adjusts to accommodate unique environments, taking into consideration nutrient gradients, oxygen supply, and water availability. Ultimately, c-di-GMP regulates the transition from motile to sessile attachment through modulation of mannose sensitive hemagglutinin(mshA)[8]. MshA pili acts as a break, tethering to chitin surfaces and triggering irreversible attachment and secretion of VPS (vibrio polysaccharides)[7].

Following secretion, Vibrio Polysaccharides bind to matrix proteins, playing an essential role in the structure of biofilm in *Vc*. Monosaccharide analysis reveals that VPS structure is characterized primarily by the polysaccharides glucose and galactose[9]. The biosynthesis of VPS is controlled by gene clusters VPS-I and VPS-II, the presence of which is necessary for biofilm formation[9]. Following VPS biosynthesis, RbmA, an essential matrix protein which facilitates cell to cell interactions, is then expressed (Figure 1)[9]. This matrix protein crosslinks with VPS, binding sister cells as they divide and grow[9]. Other matrix proteins RbmC and Bap1 ensure surface adhesion in *Vc* biofilms through cell to substrate interactions facilitated by crosslinks with VPS[9].

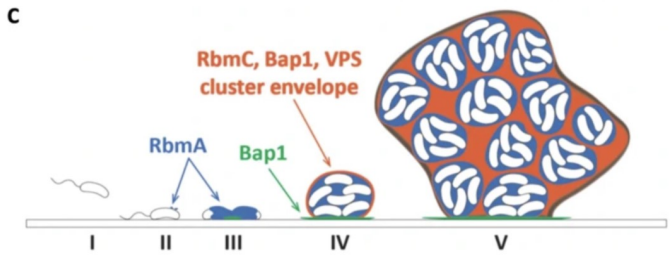


**Fig. 1** Model of *Vc* biofilm structure and matrix proteins. 3D depiction *Vc* biofilm depicts interactions between cell clusters and the role of VPS, RbmA, Bap1, and RbmC in biofilm architecture. This figure is taken from Tai, et al. (2023) who adapted imaging and data from Berk et al. (2012).

Biofilm growth occurs primarily on the edges of biofilm as opposed to the center due to a variety of factors including nutrient distribution, quorum sensing, and temperature[10]. Lower cell densities at biofilm edges trigger the production of vps through the quorum sensing–the suppression of HapR under the presence of active LuxO–thus leading to additional growth[11]. However, as the biofilm continues to expand, limited surface area causes mechanical stress, both radial and tangential[10]. Whilst radial stress is partially relieved due to biofilm growth in outer regions, tangential stress continues building up without any outlet[10]. This asymmetry results in tangential instability, leading to radial wrinkling and delamination perpendicular to the interface. To relieve tangential stress, one theory of mechanical instability suggests that wrinkling occurs where the biofilm buckles out of the growth plane and deforms together with the substrate[10]. As biofilms possess finite adhesive strength, delamination can occur subsequent to wrinkling[10]. Blisters emerge between the biofilm and substrate, merging together and causing the biofilm to separate from the substrate[10]. Alternatively, rugose phenotypes have been observed to form under the presence of mutated hapR and CytR genes. Mutations in these genes, linked to the quorum sensing process in *Vc*, promote overproduction of EPS and thus formation of rugose colonies[11]. A decrease in cellular c-di-GMP levels, which can be caused through temperatures above 30 C, also has been observed to diminish rugose phenotypes in *Vc* biofilm[11]. Regardless of cause, these rugose structures formed by wrinkling and delamination increase the resistance of biofilm against environmental stress. Under pH conditions of 4.5 for roughly 30 minutes, a majority of planktonic cells, lacking rugose biofilm structures, were killed as opposed to *Vc* cells with rugose biofilms which were 1000-fold more resistant to acidity[12]. Such acid resistance was destroyed upon the destruction of biofilm structure, suggesting that rugosity and *Vc* biofilm morphology confer acid resistance rather than individual cells[12].

This study analyzes the impacts of anthropogenic pollution on VPS and its role in biofilm development through condensing various studies. Despite being able to tolerate a range of acidities, *Vc*'s preference for alkaline ocean waters (pH 8) leads to the potential of decreasing pH level to be directly correlated with decreased biofilm growth and formation. Additionally, this paper demonstrates fluctuations of carboxyl/carbonyl group content, essential groups in VPS structure, under changing acidities. By linking this to the impacts of mildly acidic pH on biofilm formation this paper hopes to shed light on the key role of VPS in this complex relationship.

## Analysis

Previous studies model the correlation between human population density and CO2 emissions, showing that until the late 1960s both had increased super-exponentially[13]. However, within the last decade human population growth has averaged 1% per year while carbon dioxide emissions have averaged a growth rate of 2% per year[13]. Despite such numbers suggesting a complex relationship between human population and CO2 emissions, it remains clear that there remains a strong positive correlation. As depicted below in (Fig 4) the role of an increasing population density is directly correlated to increasing acidity. Areas of high population density in major cities overlap with coastal regions of low pH as compared to the global average. According to previous studies among greenhouse gases, carbon dioxide emissions are most affected by human activities and thus changes in human population density[14]. With the global population increasing by 300% and atmospheric CO2 concentration increasing by 25% within just the last 125 years, the addition of excess carbon dioxide into seawater as a result of anthropogenic

pollution has triggered the current decrease in pH[15]. Compared to pre-industrialization measures, ocean surface pH levels have decreased by ∼0.11 ± 0.03 in 2000 since 1770[16].

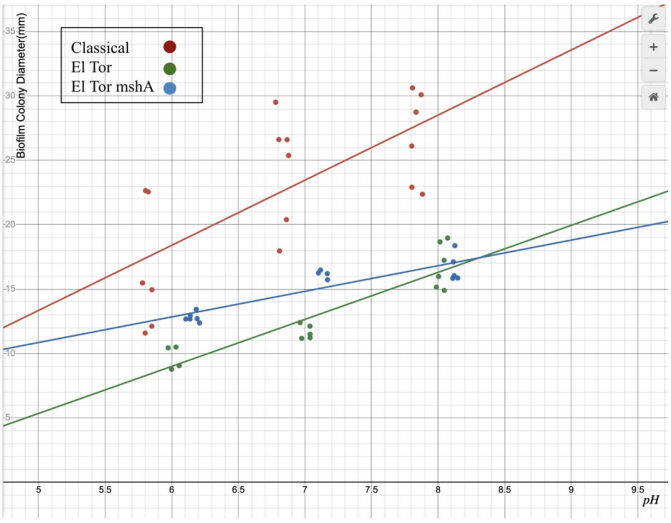


**Fig. 2** Scatter plot of observed biofilm colony diameters under changing pH conditions. Linear regressions of format y1=mx1+b fitted to each set of data (classical, El tor without mshA, and El tor with mshA). The resulting equations are y=5.06x-11.9, y=1.99x+0.92, and y= 3.6x-12.9 respectively.

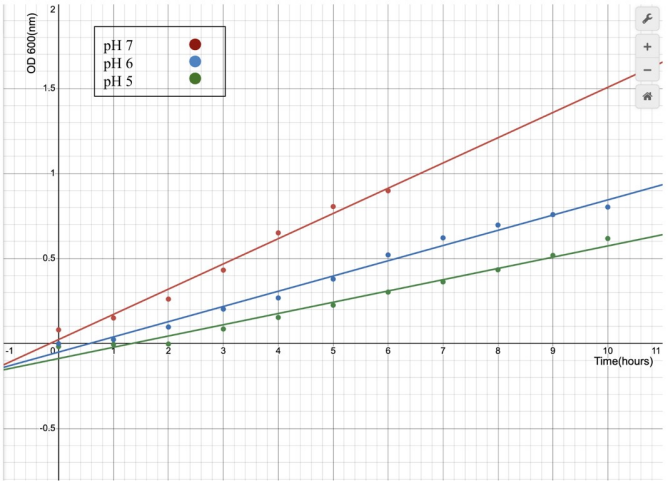


**Fig. 3** Scatter plot of recorded optical density in nanometers as time passes in hours. Linear regressions done for each separate set of data (pH 5, pH 6, pH 7) in format y1=mx1+b. The resulting equations yield y=0.066x-0.088, y=0.089x-0.051, and y=0.148x+0.023 respectively.

In order to measure the impacts of pH on biofilm colony growth, Nhu et al. grew Classical 0395 and El Tor C6706 strains of *Vc* in varying acidities[4]. Nhu et al. developed three different biofilm colonies on prepared plates of M9 salt supplemented

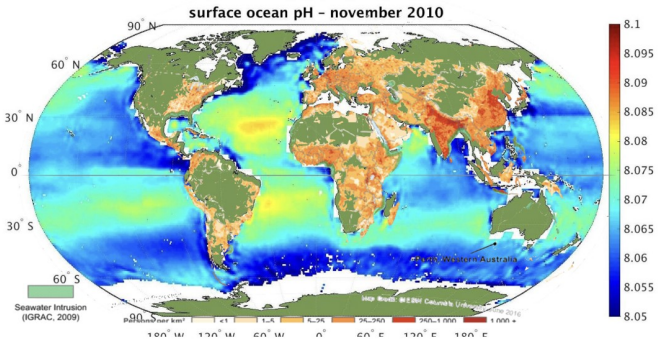


**Fig. 4** Graph of population density (expressed in person per km$^2$) layered over graph of ocean pH levels. Figure made with alterations from graphs by Costall et al. (2015) and data from the European Space Agency.

with 0.3% agar, pyruvate, and tryptone[4]. They inoculated 5 $\mu$L of saturated liquid culture onto each agar plate after growing *Vc* shaking at 200 rpm in liquid cultures of 37 C[4]. In order to also determine the impacts of mshA (mannose sensitive hemagglutinin) pili on biofilm morphology, mshA expression was inactivated through the recombining of genomic DNA for mutant EC4926 in one El Tor C6706 biofilm while another El Tor biofilm was used as a control group[4]. For the purpose of this experiment, Nhu et al. varied levels of acidity between pH6, ph7, and pH8 at a constant temperature of 37 C[4]. They then measured the diameter in millimeters of the resulting biofilm colonies grown on the M9 substrates after an incubation period of 12 hours[4]. In their study, they graphed pH against diameter in millimeters, compiling the data from all three biofilm colonies into one graph[4].

*Vc* biofilm colonies appear to spread at less rapid rates under acidic conditions. Extracted data from Nhu et al., demonstrated a positive correlation between pH and biofilm diameter(mm) in Classical 0395 strains with a slope of 5.06($r^2$=0.5, p¡10e-4) (Fig 2). Similarly, El Tor C6706 (with mshA expression) data yielded a growth rate of 3.65($r^2$=0.83, p¡10e-4) (Fig 2). Variations without mshA expression maintained a positive growth rate, although they appeared to exhibit less correlation between the two factors of pH and biofilm diameter, with a slope of 1.98($r^2$=0.78, p<10e-4) (Fig 2). Overall increasing acidity or H+ ion content decreased the growth of biofilm colonies.

Similarly, Hommais et al. shows a positive correlation between increasing pH and bacteria growth in the Ogawa 0395 strain, as demonstrated in (Fig 5). Hommais et al. studied Ogawa 0395 strain growth in a M9 medium supplemented with 0.4% glycerol and 0.1% casamino acid[17]. They maintained a steady temperature of 30.7 C while varying the acidity from pH 5, pH 6, to pH 7. Hommais et al. cultivated bacteria initially to stationary phase in LB medium of pH 6 or pH 7[17]. This biofilm was then resuspended in the same media at an OD of 600 nm, and added to 300 $\mu$L of LB in borosilicate glass tubes

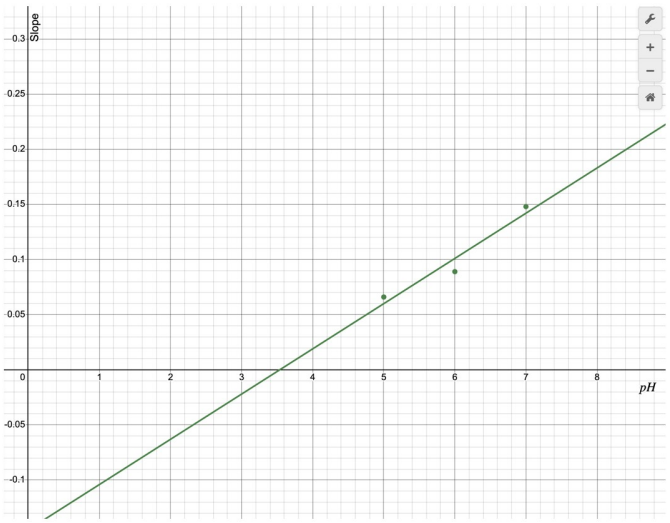


**Fig. 5** Scatter plot of recorded slopes of time(hours) vs. optical density(nanometers) as pH changes from 5-7. Linear regressions done for this set of data in format y1=mx1+b. The resulting equations yield y=0.041x-0.145($r^2$=0.94).

at a dilution of 1:100 where they were then incubated for 90 hours F[17]. Tubes were then rinsed with water before being filled with crystal violet stain for a period of 15 minutes[17]. In order to quantify the resulting optical density the bacteria associated tubes were resuspended with a 3 hour incubation period in 100% ethanol with an OD of 570 nm[17]. After the suspension period, Hommais et al. took data from 0 to 10 hours, where the data on the optical density of the biofilm was measured on an hourly basis with a wavelength of 600 nm[17].

Initially, extracted data correlates hours (0-10) with optical density in nanometers. Extracting a slope representative of such a correlation results in a growth rate of 0.066 at pH 5($\sigma$=0.188, Cl=0.25±0.11) (Fig 3). Similarly, the slope is 0.089 at a pH of 6($\sigma$=0.28, Cl=0.40±0.167) and 0.148 at a pH of 7($\sigma$=0.36, Cl=0.651±0.212) (Fig 3). When pH is graphed against these slopes, a positive correlation with slope 0.047($r^2$= 0.9376) as depicted in (Fig 5) is revealed. Thus, it can be concluded that decreasing pH, caused by increased CO2, is directly correlated with stunting the growth of bacteria in *Vc* Ogawa 0395.

## Discussion

Among the many pH sensitive chemical structures essential to *Vc* biofilm formation, carboxyl groups(a combination of carbonyl and hydroxyl groups attached to a single carbon atom), are highly reactive to changing acidities[18]. Imaging by Patel et al. downe through TEMPO scans shows the relationship between oxidation time (0-48 hours) and content (mmol $kg^{-1}$) of carbonyl or carboxyl groups[18]. Testing acidity levels varying between 5 and 7 they graphed the resulting fluctuations in carbonyl/carboxyl content[18]. NMR Spectrum imagining demonstrates the composition of the ECM, primarily made up of VPS, as containing carbonyl groups that account for 16% of carbon contributions to the C CPMAS spectrum[19] Analysis of depolymerized VPS structure reveals the presence of carboxyl groups in VPS structure[15]. Monosaccharide analysis of depolymerized VPS reveals glucose, galactose, LD-heptose, glucosamine, and perosamine as the major building blocks of VPS[20]. Further studies reveal the presence of a free carboxyl group linked to a guluronic acid bound with a glycine adduct in VPS structure[15]. Thus, fluctuations in carboxyl group content show correlations with VPS structure and its ability to crosslink with matrix proteins Bap1, RmbA, and RbmC[20].

By visualizing the interaction between VPS polysaccharides and Bap1 proteins, VPS is observed docked manually in the B-prism cavity of the protein[15]. Furthermore, although analysis on Bap157 was unable to fully image the interactions during the docking, data from Kaus, et al. suggests a preference for binding with anionic polysaccharides with linear backbones[15]. This points to the essential role of the free carboxyl groups linked to guluronic acid in the acetylated linear polysaccharide structure of VPS[15]. An additional attractive feature of this model based on PyMOL imaging by Kaus, et al., is the potential for the free carboxyl group of VPS to form a salt bridge with nearby lysine residues, further strengthening the crosslink between VPS and Bap1[15]. X-ray imaging also reveals polar and nonpolar interactions including hydrogen bonding between the Bap-1 B-prism domain and citrate carboxylate groups[15]. Such imaging further strengthens the biochemical argument that carboxyl group interactions govern VPS crosslinking with Bap-1. However, as only biofilm forming *Vc* cells facilitate Bap1-VPS crosslinking, biofilm forming cells segregate from non-forming ones. Such a phenomena of cell-VPS repulsion may be facilitated through the electrostatic tension formed by the C6 carboxylate group of L-gulose moiety in VPS and the cell surface containing a negative charge[21]. As RbmC shares a B-prism cavity structure with Bap1, carboxyl groups are likely to be essential to RbmC/VPS interactions as well[15]. Although it remains uncertain through which chemical reactions RbmA binds VPS it is known that the structural integrity of VPS, which relies on carboxyl groups, is essential when binding to the FNIII-2 domain[15].

The above correlation suggests possible impacts of VPS structural changes on the morphology and subsequent rugosity of biofilm colony structure. Blister formation, involving changing interfacial structures, is directly correlated to changing interfacial energies governed by RbmC/Bap1 in biofilm formation[10]. In Δ RbmC Δ Bap1 *Vc* variants skip the wrinkling stage, preceding directly to delamination[10]. They exhibit star shaped blister formations which collapse into one another, ultimately joining together, as opposed to the individual and isolated blisters formed by unmodified strains[10]. Tracking of Δ RbmC Δ Bap1Δ RbmA mutant biofilms show a lack of surface features, in which

the biofilm remains circular[10]. However, due to limited current research on the direct causative effects of pH on VPS structure, definitive conclusions on this topic are unable to be drawn.

This paper has, however, its limitations both with respect to data availability and the constraints of laboratory monitored experiments. Although this paper has established a strong correlation between the impacts of decreasing pH on biofilm growth in *Vc*, unaccounted factors in non-experimental environments may leave significant impacts on the results. Limitations include less control over external factors including rising temperatures, pollution, and the complex relationships between aqueous organisms. At higher temperatures- 37 C rather than 22 C- increased gene expression in biofilm regulating genes was observed. The decreased concentration of BipA, a protein degraded by higher temperatures, increases the rugosity of *Vc* biofilms[?]. Additionally, past studies have demonstrated a correlation between salinity and *Vc* biofilms with optimal growth occurring at 25% salinity[22]. These factors, unaccounted for in this review, will limit the extent to which changing acidity will affect *Vc* outside of laboratory conditions. Further limitations include additional factors inhibiting biofilm growth such as the inhibition of protein and enzyme production in mildly acidic environments. Several proteins including rfAF, O-antigen, and oligosaccharide involved in the biosynthesis of lipo-polysaccharides (LPS) yielded decreased concentrations at pH 6 as compared to pH 7[17]. Reduction of LPS concentration yields less effective cell membrane formation and thus increased membrane susceptibility to hydrophobic substances[17]. Proteins governing intermediary metabolisms in *Vc* are also affected by decreased pH. Moreover, despite showing correlation between carboxyl group content and VPS structure, current research fails to demonstrate the causative relation between pH and the failure of VPS to establish rugose biofilm. Regarding such limitations, future work should address the direct mechanisms of how acidity morphs VPS structure using SEM scans. In addition, future works could address alterations in the development of *Vc* in the context of its relations with other relevant organisms. In addition, further experimentation with changing carboxyl group content in VPS structure to observe direct changes in VPS interactions with matrix proteins will yield interesting results.

Despite such limitations this paper serves to clearly define the possible implications of anthropogenic pollution on *Vc* biofilm formation. Linking the changes in acidity to carbonyl/carboxyl group content fluctuations, this review highlights its correlation with changing VPS structure and the subsequent decrease in biofilm colony and bacteria growth.

Home to 2.2 million (+/-0.18million) species and highly complex ecosystem dynamics, even slight changes in ocean acidity hold the potential to shape the behavior and survival of marine organisms. Although not uniformly distributed, a global decrease in pH triggered by human actions and population greatly impacts *Vc* growth. Although one of many species residing in the ocean, drastic changes in *Vc* biofilm growth, when coupled with other factors that influence epidemiology, can lead to potential public health crisis and ecosystem instability.

## Methods

For the purpose of this study, data points were extracted from a graph of pH against diameter in millimeters from Nhu et al. which compiled data from all three biofilm colonies, rounding our estimates to three significant figures[4]. Such extraction was done through LoggerPro Image Analysis. In order to extract precise measurements for both the diameter (the y-axis) and the pH(x-axis), despite the two measurements being on different scales two rounds of analysis were done. To set up x-axis analysis the scale utilized was drawn on the x axis between pH 6 and pH 7 and set to a value of 1. As the origin for this graph was set to (6,0), each extracted x-point was increased by six. For y-analysis the scale was drawn between 10 and 15 mm and set to a value of 5. Using (0,10) as the origin each y-value was increased by 10 to account for this shift. With this extracted data a separate regression was constructed for each of the three strains of *Vc* on the same set of axes, plotting pH against diameter (Fig 2). Utilizing linear regressions, a line of best fit was assigned to each graph from which the slope and correlation were then extracted. With these extracted slopes, the relationship between the three various strains of *Vc* with biofilm colony growth rates was demonstrated.

Additionally, data was extracted from Hommais et al.[17]. Utilizing Logger Pro Image Analysis data was extracted from the y coordinates of the original graph. The scale used was set between 0.1 to 1 at a value of 0.9 while the origin was set to (0, 0.1). To account for the shifted graph each extracted y-value was increased by 0.1. As the x-coordinates were evenly spaced by the hour from 0-10 it was not necessary to utilize image analysis for the x component. Using this extracted data, a graph depiction of the relationship between time in hours and optical density in nanometers was constructed (Figure 3). By plotting the graph representing pH5, pH6, and pH7 on the same set of axes this paper then examined the difference in slopes between varying pHs. In addition, for the purpose of this study, due to the limited nutrients available in the M9 medium as bacteria growth approaches the limit and to avoid the impacts of plateau-phase growth on our overall data, the last four points of data of *Vc* growth in pH7 were cut out.

For the purpose of this literature review, the primary databases used were google scholar and PubMed. Keywords including vibrio cholerae, anthropogenic pollution, acidity, biofilm, VPS, and surface proteins were initially used. Upon further research words such as carboxyl, carbonyl, and rugosity were added. This literature review includes 24 papers written in English spanning from 1992 to the present day.

### Acknowledgments

Author acknowledges support from Dr. Alexis Moreau during the writing of this paper

### Data Availability Statement

Data sharing is not applicable to this article as no new data was created or analyzed in this study

### Author Biography

Meg Xu is currently in her junior year at Phillips Exeter Academy. She was two when she moved from Beijing to California, where she spent the next eight years of her life. During her time on the coast she developed a love and curiosity for the ocean and natural environments of the world. Throughout the past few years of her life she has attended Columbia Climate School, traveled to Costa Rica to assist with endangered species protection, and worked with members of the Woods Hole Oceanographic Institute to do field work/take samples. At school Meg is passionate about biology-genetics in particular. She also enjoys working in the lab, having spent a few weeks at John Hopkins learning how to do labs including gel electrophoresis and pGLO bacterial transformations.

## References

1 M. Kabir, U. Habiba, W. Khan, A. Shah, S. Rahim, P. Escalante, Z. Farooqi, L. Ali and M. Shafiq, *Climate change due to increasing concentration of carbon dioxide and its impacts on the environment in the 21st century: A mini review*.

2 J. Nhu, H. Wang and Y. Dufour, *Alkaline pH increases swimming speed and facilitates mucus penetration for Vce*.

3 D. Mora, S. Adl, A. Simpson and B. Worm, *How many species are there on Earth and in the ocean?*

4 T. Santos, L. Alvarez and B. Sit, *BipA Exerts Temperature Dependent Translational Control of Biofilm Related Colony Morphology in Vibrio Cholerae*.

5 J. Klose, *Differential regulation of multiple flagellins in Vce*.

6 J. Teschler, C. Nadell, K. Drescher and F. Yildiz, *Mechanisms underlying Vce biofilm formation and dispersion*.

7 R. Utada, J. Fong, M. Gibiansky, F. Yildiz, R. Golestanian and G. Wong, *Vce use pili and flagella synergistically to effect motility switching and conditional surface attachment*.

8 A. Jones, K. Davis, W. Thongsomboon, D. Sanchez, V. Banakar, L. Cegelski, G. Wong and F. Yildiz, *C-di-GMP regulates motile to sessile transition by modulating MshA pili biogenesis and near-surface motility behavior in Vce*.

9 M. Tai, J. Yan and C. Waters, *New insights into Vc biofilms: From molecular biophysics to microbial ecology*.

10 J. Yan, C. Fei, S. Mao, A. Moreau, N. Wingreen, A. Kosmrlj, H. Stone and B. Bassler, *Mechanical instability and interfacial energy drive biofilm morphogenesis*.

11 B. Hammer, *Quorum Sensing Controls Biofilm Formation in Vibrio Cholerae*.

12 J. Zhu and J. Mekalanos, *Quorum Sensing Biofilms Enhance Colonization in Vibrio Cholerae*.

13 J. Yeh and C. Liao, *Impact of population and economic growth on carbon emissions in Taiwan using an analytic tool STIRPAT*.

14 D. Hüsler, *Human population and atmospheric carbon dioxide growth dynamics: Diagnostics for the future*.

15 A. Kaus, E. Chupp, J. Lu, C. Visudharomn and R. Olson, *The 1.9 Å crystal structure of the extracellular matrix protein Bap1 from Vce provides insights into bacterial biofilm adhesion*.

16 B. Jiang, R. Feely, S. Lauvset and A. Olsen, *Surface ocean pH and buffer capacity*.

17 C. Hommais, V. Labas, E. Krin, C. Tendeng, O. Soutorina, A. Danchin and P. Bertin, *Effect of mild acid pH on the functioning of bacterial membranes in Vce*.

18 R. Patel, D. Haltrich, T. Rosenau and A. Potthast, *Studies of the chemoenzymatic modification of cellulosic pulps by the laccase-TEMPO system*.

19 J. Reichhardt, F. Yildiz and L. Cegelski, *Characterization of the Vibrio Cholerae Extracellular Matrix: A Top-Down Solid-State NMR Approach*.

20 J. Yildiz, I. Sadovskaya, T. Grard and E. Vinogradov, *Structural characterization of the extracellular polysaccharide from Vce O1 El-Tor*.

21 D. Moreau and A. Hinbest, *Surface remodeling and inversion of cell-matrix interactions underlie community recognition and dispersal in Vibrio cholerae biofilms*.

22 R. Singleton, S. Jangi and R. Colwell, *Effects of Temperature and Salinity on Vibrio Cholerae Growth*.

 